J. Phys. D: Appl. Phys. **45** (2012) 012001 (5pp) doi:10.1088/0022-3727/45/1/012001

FAST TRACK COMMUNICATION

Aerogel and ferroelectric dielectric materials for plasma actuators

Ryan Durscher and Subrata Roy

Applied Physics Research Group, Department of Mechanical and Aerospace Engineering, University of Florida, Gainesville, FL 32611-6300, USA

E-mail: roy@ufl.edu

Received 15 July 2011, in final form 21 November 2011
Published 9 December 2011
Online at stacks.iop.org/JPhysD/45/012001

Abstract

This paper presents performance evaluation of two thick materials with extreme permittivity as dielectric barrier discharge actuators. Specifically, the use of silica aerogels and ferroelectrics is investigated. Due to high polarizability of the ferroelectric material the supplied power manifests itself primarily as heat generation with no measurable thrust. The silica aerogel, however, has a significant impact on thrust saturation as compared with other dielectrics reported to date. Specifically, the silica aerogel is found to have an order of magnitude better thrust to actuator weight ratio than acrylic and twice than that of Kapton with no power penalty, making it potentially useful for small vehicle applications.

(Some figures may appear in colour only in the online journal)

In its simplest form a dielectric barrier discharge (DBD) plasma actuator consists of two conducting electrodes placed asymmetrically on either side of a dielectric material. Upon application of a sufficiently high ac voltage across the electrodes, a thin layer of weakly ionized plasma forms on the surface of the dielectric. The plasma imparts an electro-hydrodynamic (EHD) body force on the neutrally charged ambient air inducing a tangential wall jet through a collisional energy transfer mechanism that is yet to be understood.

Exploration for the aerodynamic benefits of the induced body force from these actuators grew exponentially since it was first publicized in the mid-1990s. Roth *et al* [1] used a DBD actuator to manipulate the boundary layer on a flat plate over a range of free-stream velocities. Since then these actuators have been used as control devices in airfoils [2, 3], landing gear noise reduction [4], low-pressure turbine blades [5] and bluff bodies [6]. As continued progress is made in the DBD actuator design there is no doubt that new applications will continue to emerge.

Much of the progress that has been made stems from parametric studies which have focused on aspects such as applied voltage/frequency, dielectric material, electrode arrangement and geometry in an effort to achieve an optimized device [7–12]. This paper explores materials with extreme relative dielectric constants (ε_r). Specifically, the performance of several millimetre thick slabs of silica aerogels and ferroelectric dielectrics in the DBD design is investigated. The nominal dielectric constants for these two materials are at the extreme ends of dielectric properties with their respective relative dielectric constants being ∼1.2 and 1750. The low density of the silica aerogel and its operational impact on the actuator's weight are also demonstrated and discussed.

A DBD actuator and its powering circuit are shown schematically in figure 1. The actuator consists of two linear electrodes (∼70 μm thick copper tape) separated by a dielectric medium (figure 1(*a*)). The exposed electrode has a width w_1, while the lower electrode is extended to a width w_2. There is no horizontal displacement between the electrodes. Each electrode is supplied with a high voltage, 14 kHz sinusoidal signal from a Tektronix AFG3022B with the waveform supplied to the lower electrode having a 180° relative phase shift. The waveforms are further amplified by a dual output audio amplifier (QSC RMX 2450) which is then stepped up using Corona Magnetics high-voltage transformers (figure 1(*b*)). The voltage and current supplied to the actuators are monitored using high-voltage (Tektronix P6015A) and

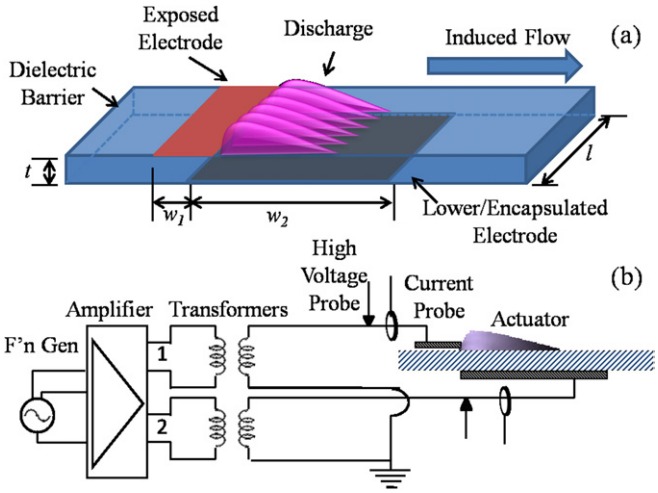

Figure 1. Schematics of (*a*) the dielectric barrier plasma actuator and (*b*) the dual powered circuit.

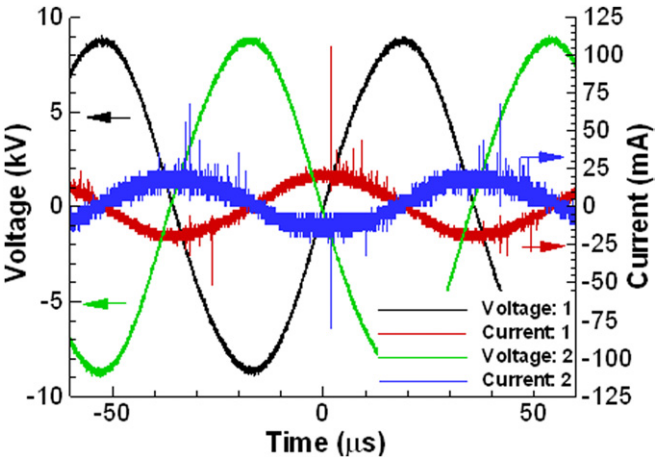

Figure 2. Representative example of voltage and current waveforms during actuator operation. The dielectric used is a 6 mm thick silica aerogel.

current probes (Pearson Electronics 2100) with the signals being captured using a digitizing oscilloscope (Tektronix DPO3014). Representative example waveforms for this setup are shown in figure 2 for a 6 mm thick silica aerogel actuator. The individual powering branches (as shown in figure 1(*a*)) are numerically represented as channels 1 and 2. For each test case, the mean power delivered to the plasma is calculated by averaging the product of the instantaneous voltage and current over 200 periods. To test a wider range of frequencies, a high-voltage amplifier (Trek 30/20C) is used, replacing the transformers and audio amplifier shown in figure 1(*b*) with the lower electrode grounded.

In a prior experimental investigation, Thomas *et al* [12] showed that for a fixed plate thickness and frequency, the saturation thrust (or maximum force achieved) decreased as the dielectric constant increased from 2 to 6. To test the upper extreme of dielectric permittivity, we investigate the use of a ferroelectric (modified lead zirconate-titanate, PZT) material as a dielectric. The ferroelectric sample has a nominal relative dielectric constant of 1750. The dimensions of the ferroelectric sample are 40 mm × 12 mm × 3 mm (x, y, t). The width of

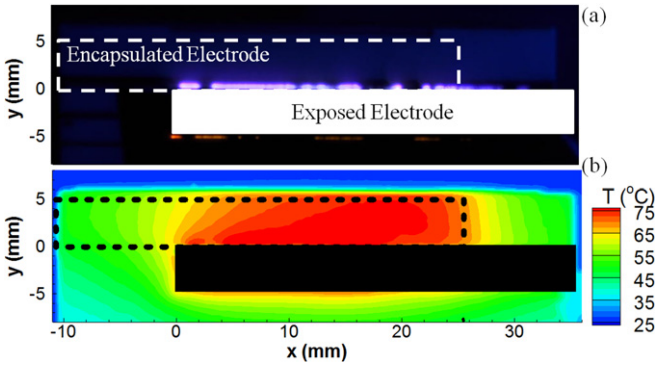

Figure 3. (*a*) Picture of plasma discharge and (*b*) the corresponding surface temperature for a 3.5 kVpp, 5 kHz sinusoidal input. Temperature measurement is taken after 300 s of operation.

the exposed and encapsulated electrodes for the ferroelectric sample are $w_1 = w_2 = 5$ mm.

The ferroelectric material allowed for a discharge ignition at a much lower input voltage as compared with materials of similar thickness with lower dielectric constants. A representative picture of the discharge generated is shown in figure 3(*a*) for an input voltage of 3.5 kVpp at 5 kHz. As shown in the figure, the discharge is concentrated around the exposed electrode's edge. At higher voltages (>5 kVpp, 5 kHz), for this thickness of ferroelectric, dielectric heating became a problem with temperatures reaching ~200 °C after only tens of seconds of operation. At this point, keeping the adhesively backed copper tape electrodes adhered to the surface was difficult. Even at these higher voltages the discharge never appears to propagate downstream as would an actuator constructed from a lower dielectric constant. This may be due to the high surface charge accumulated from spontaneous electron emission from the polarizable ferroelectric material. This could modify the surface potential and the electric field locally, which could limit the expansion of the plasma along the surface. An Ohaus precision balance (Adventurer™ Pro AV313C, resolution 1 mg) is used to quantify any measurable thrust. The actuators are mounted to the scale by an acrylic stand that protrudes though a small opening in a Faraday's cage. The cage is used to shield the balance from any electromagnetic noise present due to the high electric fields required to generate the plasma discharge. Since the thrust produced is directly tied to the voltage, over the range of inputs tested (1.5–3.5 kVpp at 14 kHz) no measurable force was detected.

With no force being achieved, the dielectric heating of the device was investigated. A FLIR A320 infrared camera was used. The camera has a spectral range of 7.5–13 μm and a pixel resolution of 320 × 240 pixels. The ambient humidity (55% RH), distance from the actuator (0.33 m) and material emissivity were considered in determining the surface temperature. The emissivity of the ferroelectric material was found to be 0.96 ± 0.02 and was determined by heating the dielectric to a uniform temperature and comparing the camera's readout with a surface mounted thermocouple. As mentioned in the previous paragraph, the high temperatures observed during initial tests were found to exceed the boundaries set by the current actuator configuration; as such, the operational

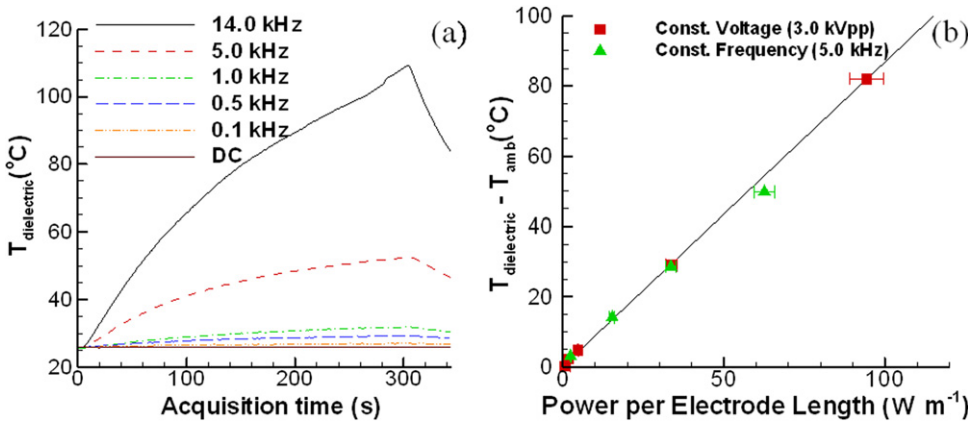

Figure 4. (*a*) Surface temperature as a function of time about point 12.5 mm, 1.5 mm (*x*,*y*) for varying frequencies and (*b*) temperature rise in the dielectric after 300 s of actuation for a modulated frequency at 3 kVpp (red square) and a modulated voltage at 5 kHz (green diamond) as a function of power per unit length of the electrode.

voltage/frequency regimes were set so as not to exceed these limits. Temperature measurements were made over a range of voltages (1.5–4 kVpp) at 5 kHz as well as over a range of frequencies (dc to 14 kHz) at 3 kVpp. Figure 3(*b*) shows a representative surface temperature distribution after 300 s of operation. Looking at a time trace (figure 4(*a*)) for a point taken at $x = 12.5$ mm and $y = 1.5$ mm we see that the surface temperature shows a sharp initial increase and then gradually rises to a steady-state temperature. The profiles presented in figure 4(*a*) are consistent with that of Joussot *et al* [13]. The measurements shown in figure 4(*a*) correspond to an initial 5 s of non-actuation after which the device was turned on for 300 s. Once turned off, another 40 s of data acquisition continued. Noting the seemingly strong dependence on frequency, a plot of the temperature rise after 300 s (at $x = 12.5$ mm, $y = 1.5$ mm) as a function of power shows a linear relationship proportional to $0.87\,^{\circ}\mathrm{C\,W^{-1}\,m}$ (figure 4(*b*)). This proportionality is independent of the input frequency and voltage, a trend also observed by Joussot *et al* [13]. However, as shown in figure 4(*a*), for a constant voltage one may reach the same surface temperature faster using a higher frequency. The results indicate a possibility of operating at an even higher frequency to generate thermal loading on a faster timescale. The same argument can also be made for a constant frequency with a modulated voltage.

Silica aerogel was used to investigate the low end of the dielectric spectrum. In general, silica aerogels consist of a complex microstructure of silicon dioxide in which air occupies majority of the volume. For the samples tested, ~95% of the dielectric's volume was air resulting in a density ranging from 0.04 to $0.12\,\mathrm{g\,cm^{-3}}$ with results being reported for samples having a density of $0.11\,\mathrm{g\,cm^{-3}}$. Silica aerogels in this range of densities have a relative dielectric constant of 1.1–1.2 [14]. The sample of aerogel used in this work is shown in figure 5(*a*) along with an inset image of a plasma discharge being ignited on a smaller sample as a proof of concept demonstration. For the silica aerogel tests, the electrode widths were $w_1 = 5$ and $w_2 = 20$ mm.

The surface morphology of the silica aerogel actuators obtained using non-contact atomic force microscopy (AFM) is shown in figure 5(*b*) for a $5\,\mu\mathrm{m} \times 5\,\mu\mathrm{m}$ surface area. The arithmetic mean surface roughness (S_a) ranged from 15 to 102 nm over three randomly selected surface areas of 4, 25 and $100\,\mu\mathrm{m}^2$. Relative to the thickness of the exposed copper electrode (~$70\,\mu$m) the measured surface roughness was at least an order of magnitude smaller. Presumably the distributed roughness of the aerogel material will have less influence inside the boundary layer as compared to the thickness of the electrode. The effects of the inhomogeneous accumulation of surface charge due to the surface roughness were not investigated. Such a phenomenon may affect the overall structure of the plasma formation. However, the temporal characteristics of the discharge current for the silica aerogel actuators (shown in figure 2) are consistent with those reported in the literature [15]. Large irregular spikes in the current, indicative of cathode direct streamers [16], are observed during the positive slope of the voltage supplied to the exposed electrode. During the downward negative slope of the supplied voltage the plasma is observed to operate in a more diffuse mode [16].

The induced force produced by actuators using Kapton ($\varepsilon = 3.5$), acrylic ($\varepsilon = 3$) and aerogel dielectrics for various thicknesses are presented in figure 6. Over the range of voltages tested, no noticeable surface damage was observed for the aerogel. The open symbols found in figure 6 (and figure 7) indicate a direct thrust measurement made using the force balance described previously. The closed symbols represent force measurements inferred from a control volume analysis on the induced velocity field recorded using two-component particle image velocimetry (PIV). A representative time-averaged flow field is shown in figure 5(*c*) for a 36 kVpp input, where the dashed lines correspond to the sides of the control volume. The primary components of the PIV system are a Nd : YAG, dual-cavity pulsed, 532 nm laser (New Wave Research Solo PIV II 30) and a LaVision ImagerPro X 4M (2048 × 2048 pixels) camera. For each run, 300 image pairs are taken at a repetition rate of 7.2 Hz. The flow was seeded with Ondina oil having a mean diameter of ~$0.8\,\mu$m generated with a TSI atomizer (Model 9302). The control volume analysis used is similar to that of Hoskinson *et al*

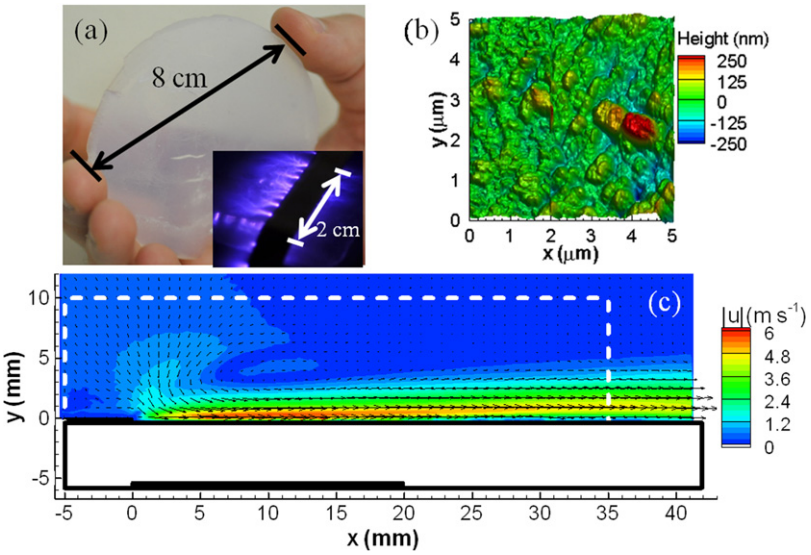

Figure 5. (*a*) Actual sample of silica aerogel used for collecting data with the inset showing a plasma discharge on a smaller sample of silica aerogel, (*b*) surface topography of the silica aerogel as measured with atomic force microscopy and (*c*) velocity distribution measured using PIV over the aerogel sample (dashed lines indicate the boundaries of the control volume considered).

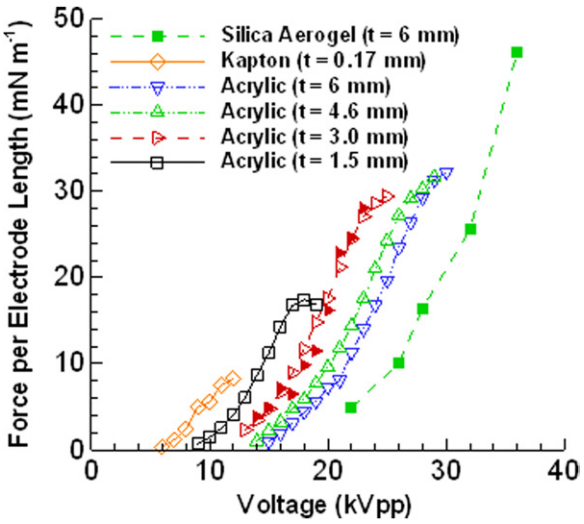

Figure 6. Effect of the dielectric thickness as a function of voltage on thrust production for actuators constructed out of silica aerogel, Kapton and acrylic (open symbols correspond to direct thrust measurements, while closed symbols are inferred from a control volume analysis on the induced flow field).

[11] though all three sides of the volume are considered here for increased accuracy. The reaction force imparted to the dielectric was calculated using the conserved form of the momentum equation in the x-direction assuming the following simplifications: time independence, constant pressure and constant air density ($\rho_{\text{air}} = 1.184\,\text{kg m}^{-3}$). A comparison between inferred and direct thrust measurements is shown in figure 6, with good agreement, for a 3 mm thick acrylic actuator.

As previously mentioned in a prior optimization study, Thomas *et al* [12] showed that for a constant thickness, higher voltages can be applied resulting in larger forces when using a material with a lower dielectric constant. This is demonstrated in figure 6, by comparing the 6 mm thick acrylic and aerogel samples. Interestingly for this frequency, the induced force for an acrylic actuator asymptotes at about 34 mN m^{-1} while the silica aerogel demonstrates a much higher thrust of 47 mN m^{-1} with no sign of saturation The voltage range tested in this study was up to 36 kVpp though higher voltages would have been possible for the aerogel actuator. It is also notable that for a given voltage the acrylic actuator generates more thrust up to its saturation point.

An added benefit of the aerogel is its low density, a parameter that would be critical when applying these actuators to medium to small/micro air vehicles. The benefits of using a thicker dielectric in the DBD actuator design have also been documented in the literature [12]. Consistent with previously reported results [12], figure 6 shows that by increasing the thickness of the dielectric layer larger voltages can be applied to the actuator. The additional voltage increases the maximum thrust that may be achieved. A disadvantage of increasing the dielectric thickness, however, is that the weight of the actuator also increases. Although this would be less detrimental for large-scale applications, it could prove critical at smaller scales seeking to benefit from the increased body force associated with thicker dielectrics. Figure 7 re-plots the data shown in figure 6 on a thrust to actuator weight ratio defined by equation (1). All dimensions are in centimetres (referring to figure 1(*a*)) and the density ($\rho_{\text{dielectric}}$) of acrylic, aerogel and Kapton were taken as 1.20 g cm^{-3}, 0.11 g cm^{-3}, and 1.42 g cm^{-3}, respectively:

$$\frac{\text{Force}}{\text{Weight}} = \frac{f}{t \times l \times (w_1 + w_2) \times \rho_{\text{dielectric}}}. \qquad (1)$$

For the conventional dielectrics tested (Kapton and acrylic) a thinner dielectric is beneficial based on a force-to-weight basis. However, when the silica aerogel is considered the benefit of this extremely low density material is evident (figure 7). Referring to figure 7(*a*), for a given thickness ($t = 6$ mm), the net force-to-weight ratio measured has increased from 1.8×10^{-2} (at 30 kVpp) to 2.9×10^{-1}

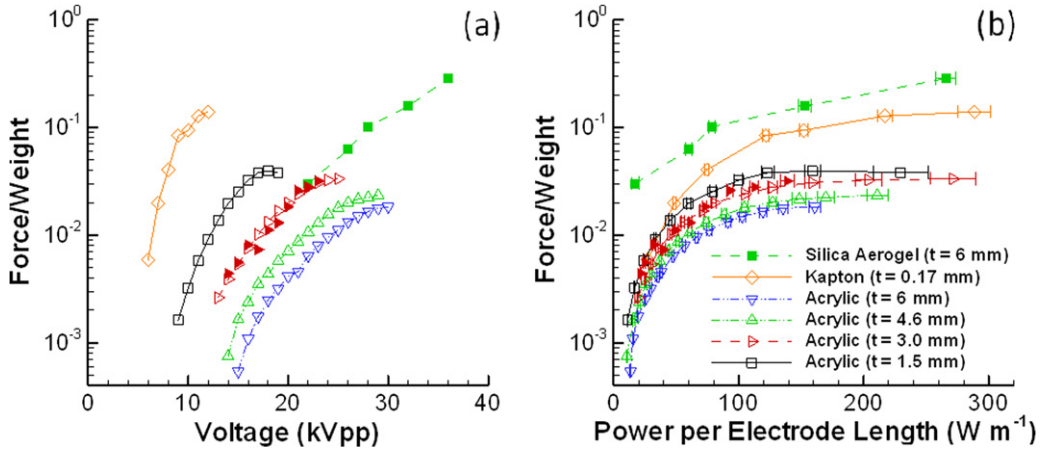

Figure 7. Ratio of force generated to the actuator weight for various dielectrics as a function of (*a*) applied voltage and (*b*) power consumption per unit length of the electrode. Actuators are constructed out of silica aerogel, Kapton and acrylic (open symbols correspond to direct thrust measurements, while closed symbols are inferred from a control volume analysis on the induced flow field).

(at 36 kVpp) for the acrylic and aerogel samples, respectively. The net force-to-weight ratio for Kapton is 1.4×10^{-1} at 12 kVpp. This increased thrust-to-weight basis comes with no added power consumption for the actuator, as shown in figure 7(*b*). Specifically, at a lower power the benefit of using aerogel as a dielectric is significant.

In conclusion, dielectrics possessing extreme relative dielectric constants of ∼1.2 (silica aerogel) and 1750 (ferroelectric) have been investigated. Silica aerogel was found to a have a strong effect on the thrust generation. Significantly higher voltages were sustainable for such a low dielectric constant compared with other materials of similar thickness. The aerogel's minimal weight penalty and higher thrusts (i.e. thicker dielectric) may be useful for practical applications such as medium to small/micro air vehicles. The friability of the current samples of silica aerogel makes them challenging for direct introduction to applications. However, the potential benefit of large improvement in thrust-to-weight ratio with no power penalty using such lightweight materials is encouraging. As such, more robust aerogels are currently under investigation. For the ferroelectric material studied, significant heating of the surface resulted while no force was observed over the range of tested voltages and frequencies. The results indicate a possibility of operating at a higher frequency (or voltage) to generate thermal loading on a faster timescale. This may have possible implementation as a heat bump in high-speed flow control applications. Thinner, high permittivity material should also be examined for thrust generation.

Acknowledgments

This work was sponsored in part under Air Force Office of Scientific Research Grants #FA9550-09-1-0372 and #FA9550-09-1-0615 monitored by Dr Doug Smith and Charles Suchomel.

References

[1] Roth J R, Sherman D M and Wilkinson S P 1998 *36th AIAA Aerospace Science Meeting (Reno, NV) AIAA Paper* No 1998-328
[2] Benard N, Braud P, Jolibois J and Moreau E 2008 *4th Flow Control Conf. (Seattle, WA) AIAA Paper* No 2008-4202
[3] Visbal M R, Gaitonde D V and Roy S 2006 *36th AIAA Fluid Dynamics Conf. and Exhibit (San Francisco, CA) AIAA Paper* No 2006-3230
[4] Post M and Corke T 2006 *AIAA J.* **44** 3125
[5] Huang J, Corke T C and Thomas F O 2006 *AIAA J.* **44** 51
[6] Sung Y, Kim W, Mungal M G and Cappeli M 2006 *Exp. Fluids* **41** 479
[7] Abe T, Takizawa Y, Sato S and Kimura N 2007 *45th AIAA Aerospace Sciences Meeting and Exhibit (Reno, NV) AIAA Paper* No 2007-187
[8] Roy S and Wang C-C 2009 *J. Phys. D: Appl. Phys.* **42** 032004
[9] Enloe C L, McLaughlin T E, VanDyken R D, Kachner K D, Jumper E J, Corke T C, Post M and Haddad O 2004 *AIAA J.* **42** 595
[10] Forte M, Jolibois J, Pons J, Moreau E, Touchard G and Cazalens M 2007 *Exp. Fluids* **43** 917
[11] Hoskinson A R, Hershkowitz N and Ashpis D E 2008 *J. Phys. D: Appl. Phys.* **41** 245209
[12] Thomas F O, Corke T C, Iqbal M, Kozlov A and Schatzman D 2009 *AIAA J.* **47** 2169
[13] Joussot R, Hong D, Rabat H, Boucinha V, Weber-Rozenbaum R and Leroy-Chesneau A 2010 *40th Fluid Dynamics Conf. and Exhibit (Chicago, IL) AIAA Paper* No 2010-5102
[14] Hrubesh L W, Keene L E and Latorre V R 1993 *J. Mater. Res.* **8** 1763
[15] Enloe C L, McLaughlin T E, VanDyken R D, Kachner K D, Jumper E J and Corke T C 2004 *AIAA J.* **42** 589
[16] Enloe C L, Font G I, McLaughlin T E and Orlov D M 2008 *AIAA J.* **46** 2730